

---

# PRAViC: PROBABILISTIC ADAPTATION FRAMEWORK FOR REAL-TIME VIDEO CLASSIFICATION

---

A PREPRINT

**Magdalena Trędownicz**

Faculty of Mathematics and Computer Science  
Jagiellonian University, Kraków, Poland  
magdalena.tredowicz@student.uj.edu.pl

**Łukasz Struski**

Faculty of Mathematics and Computer Science  
Jagiellonian University, Kraków, Poland  
lukasz.struski@uj.edu.pl

**Marcin Mazur**

Faculty of Mathematics and Computer Science  
Jagiellonian University, Kraków, Poland  
marcin.mazur@uj.edu.pl

**Szymon Janusz**

Faculty of Mathematics and Computer Science  
Jagiellonian University, Kraków, Poland  
szymon.janusz@student.uj.edu.pl

**Arkadiusz Lewicki**

Faculty of Applied Computer Science  
University of Information Technology  
and Management in Rzeszów, Poland  
a.lewicki@lptw.pl

**Jacek Tabor**

Faculty of Mathematics and Computer Science  
Jagiellonian University, Kraków, Poland  
jacek.tabor@uj.edu.pl

## ABSTRACT

Video processing is generally divided into two main categories: processing of the entire video, which typically yields optimal classification outcomes, and real-time processing, where the objective is to make a decision as promptly as possible. The latter is often driven by the need to identify rapidly potential critical or dangerous situations. These could include machine failure, traffic accidents, heart problems, or dangerous behavior. Although the models dedicated to the processing of entire videos are typically well-defined and clearly presented in the literature, this is not the case for online processing, where a plethora of hand-devised methods exist. To address this, we present PrAViC, a novel, unified, and theoretically-based adaptation framework for dealing with the online classification problem for video data. The initial phase of our study is to establish a robust mathematical foundation for the theory of classification of sequential data, with the potential to make a decision at an early stage. This allows us to construct a natural function that encourages the model to return an outcome much faster. The subsequent phase is to demonstrate a straightforward and readily implementable method for adapting offline models to online and recurrent operations. Finally, by comparing the proposed approach to the non-online state-of-the-art baseline, it is demonstrated that the use of PrAViC encourages the network to make earlier classification decisions without compromising accuracy.

## 1 Introduction

In recent years, there has been a notable increase in the utilization of convolutional neural networks (CNNs) across a range of fields where the capacity to make expeditious decisions could be crucial, including medicine [13, 18], human action recognition (HAR) [17, 28], and autonomous driving [24]. However, despite the growing prevalence of CNNs in these domains, there remains a lack of a unified approach to the problem of making early decisions based solely on the initial frames.

Conversely, numerous offline approaches have been proposed (see, e.g., [1, 7, 8, 16, 29]) to address the problem of video data classification. However, these models usually require access to entire videos, which precludes their real-time applicability. Although certain techniques have been developed to facilitate the adaptation of offline models to the online

domain (e.g., [12, 25]), there remains a need for the development of more generalizable solutions that can accommodate diverse forms of data.

To address the aforementioned gap, we propose a novel probabilistic adaptation framework for real-time video classification (PrAViC). In contrast to traditional methodologies, our approach allows for the adoption of existing three-dimensional convolutional models, wherein subtle adjustments are made to the architectures in order to retain the utility of the pre-trained classification model weights. Moreover, our strategy encompasses the recursive application of this adapted model in the real-time analysis of video data streams. This pioneering approach not only slashes the model training time by leveraging pre-existing weights but also unlocks the potential for recursive utilization. The ramifications of this advancement extend across various sectors including industry, medicine, and public safety, where swift real-time analysis is paramount for informed decision-making and proactive measures. In the experimental study, we demonstrate the efficacy of our approach when applied to a selection of state-of-the-art offline models trained on three real-world datasets, including two publicly available datasets, UCF101 [20] and EgoGesture [30], as well as a closed-access real Ultrasound dataset, comprising Doppler ultra-317 sound images representing short-axis and suprasternal views of newborn hearts. Furthermore, we introduce an innovative function that allows the model to make earlier exits (decisions) when sufficient evidence is gathered. The effect of such a function is presented in Fig. 1. By incorporating this function into the objective, the model optimizes the timing of its decisions, enhancing efficiency with a slight loss of accuracy.

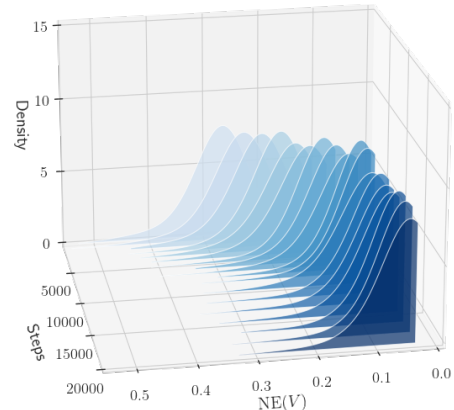


Figure 1: Progress of the model’s early decision function during training.

In conclusion, our contribution can be summarized as follows:

- we introduce PrAViC, a novel, unified, and theoretically-based probabilistic adaptation framework for online classification of video data, which has the potential to make a decision at an early stage, thus improving the efficiency of the classification process,
- we demonstrate that our solution provides a straightforward and readily implementable method for adapting offline video classification models to online and recurrent use,
- we conduct experiments which indicate that the proposed approach is capable of facilitating earlier classification decisions without compromising accuracy when compared to selected non-online state-of-the-art solutions.

## 2 Related works

While video-based 3D networks have been widely studied in offline settings [1, 7, 8, 16, 29], developing online models remains still a challenge. Such online models are able to real-time classification, enabling applications such as emergency situations detection or medical diagnostics.

**Adaptations 2D models for online video data** Given that video consists of consecutive frames, each frame can be classified individually using 2D CNN models [14]. Such an approach represents an online technique and works well as real-time classification, due to a low number of parameters. This method however might not be optimal due to the absence of temporal information from the entire video, potentially resulting in misclassifications, such as predicting "sitting down" when the action involves transitioning from sitting to standing. To develop a model capable of processing online data in real-time, researchers often opt for 2D networks supplemented with additional mechanisms to manage temporal data [3, 19, 23, 25, 27]. The authors of [25] adopted a temporal shift module (TSM). By shifting part of the channels along the temporal dimension, TSM can help capture temporal relationships.

**Online 3D models for real-time usage** Since it was proven [2], that 3D CNNs achieve better accuracies compared to 2D CNNs for video classification task, novel approaches employ differing versions of 3D convolutional kernels. Several works proposed dedicated architectures of online 3D networks [10, 13, 18, 28], which are supposed to operate in real-time. Combining 3D CNN architectures with various long short-term memory models is another commonly utilized approach. [15] introduce a DNN merging 3D DenseNet variants and BiLSTM. In [4] R2plus1D and ConvLSTM are combined in a parallel module. The proposed network utilizes the attention mechanism to extract the features that need attention in the channel and the spatial axes. Another approach [22], combines a vision transformer for human pose estimation with a CNN-BiLSTM network for spatio-temporal modeling within keypoints sequences. Attention mechanisms additionally with transformer layers were also applied in [5]. Converting various well-known

resource-efficient 2D CNNs into 3D CNNs [11] is another proposed approach. The most closely related work to ours is [12], which explores the adaptation of 3D CNNs (especially 3D ResNet family models) for online video stream processing. Köpüklü, Okan, et al. [12] employ no temporal downsampling combined with storing intermediate volumes of the architecture in a cache for use during inference.

### 3 Probabilistic Adaptation Framework for Real-time Video Classification (PrAViC)

This section presents the details of the proposed PrAViC model (**P**robabilistic **A**daptation **F**ramework for **R**eal-time **V**ideo **C**lassification). For the reader’s convenience, the problem of video classification is divided into offline and online. In the offline case, where the entire video is available, classification can be performed by processing the entire video. In the online case, where consecutive images are obtained, the objective is to make a decision using only a partial subset of the potentially available frames.

**Offline case** We commence with a description of the model for the offline case. For the sake of simplicity, we limit our discussion to the case of binary classification. We are given a video  $V = [V_0, \dots, V_n]$ , which is represented as a sequence of images  $V_i$  (frames). Then, the network  $\phi : \mathcal{V} \rightarrow [0, 1]$  returns the (soft) probability that  $V$  belongs to the positive class. The final decision is based on the threshold  $\tau$ , where typically  $\tau = 1/2$ . Thus if  $\phi(V) \geq \tau$ , we conclude that the class of  $V$  is positive.

Let us consider the case where the soft probability is unknown, but for every threshold value  $\tau$  we can deduce whether  $\phi(V) \leq \tau$ . In this scenario, one can obtain the soft probability  $\phi(V)$  as follows:

$$\phi(V) = \text{Prob}(\phi(V) \leq \tau : \tau \sim \text{unif}_{[0,1]}). \quad (1)$$

This can be interpreted as selecting a random threshold value  $\tau$  from the interval  $[0, 1]$  and calculating the probability of being below the threshold.

The subsequent paragraph addresses the question of how the offline model can be applied to the online procedure.

**Online (early exit) procedure** We describe the standard general setting for the online early exit model. We assume that the frames arrive consecutively (on occasion, we permit them to arrive in groups of, e.g., two, four, or eight). Thereafter, given a trained classification network  $\phi$  (as described in the previous paragraph), we fix a threshold  $\tau \in [0, 1]$  and proceed with the following steps:

1. start with  $k = 0$ ;
2. load  $V_k$  and compute  $p_k = \phi([V_0, \dots, V_k])$ ;
3. if  $p_k \geq \tau$ , then return class 1 (positive) for  $V = [V_0, \dots, V_n]$ ; else put  $k = k + 1$ ;
4. if  $k = n + 1$ , then stop the algorithm and return class 0 (negative); else return to step 2.

The objective of the aforementioned procedure is to allow making the decision of  $V$  being in a positive class before loading all frames from  $V$ . It should be noted that if we operate in the offline mode, where we have access to all data, the above algorithm can be constrained to computing  $p = \max\{p_1, \dots, p_k\}$ , and then determining that the class of  $V$  is negative if  $p < \tau$ , or positive otherwise.

The underlying concept of our proposed solution is that of a continuous probabilistic model for the decision threshold of activity detection. This is discussed in detail in the following paragraph.

**Probabilistic model** First, observe that once the aforementioned procedure is completed, we are only aware of the decision that has been made, but we lack the information necessary to calculate the probability of the given outcome. Without this information, it is not possible to use BCE loss and fine-tune the model. To address this issue, we apply the probabilistic concept from Eq. (1), which allows us to calculate the soft probability of the decision, given the knowledge that the decision was made for an arbitrary threshold. Then we get that the probability that  $V$  has the positive class in the online case is given by

$$p(V) = \max(p_0, \dots, p_n), \text{ where } p_i = \phi([V_0, \dots, V_i]). \quad (2)$$

This is of paramount importance insofar as our objective is for the model to make more timely decisions (see Fig. 2).

**Expected time of early exit** To proceed to the probabilistic approach, we first calculate the expected time our model makes an early exit. For a fixed video  $V$ ,  $T_V$  denotes the random variable that returns the time we have made an early

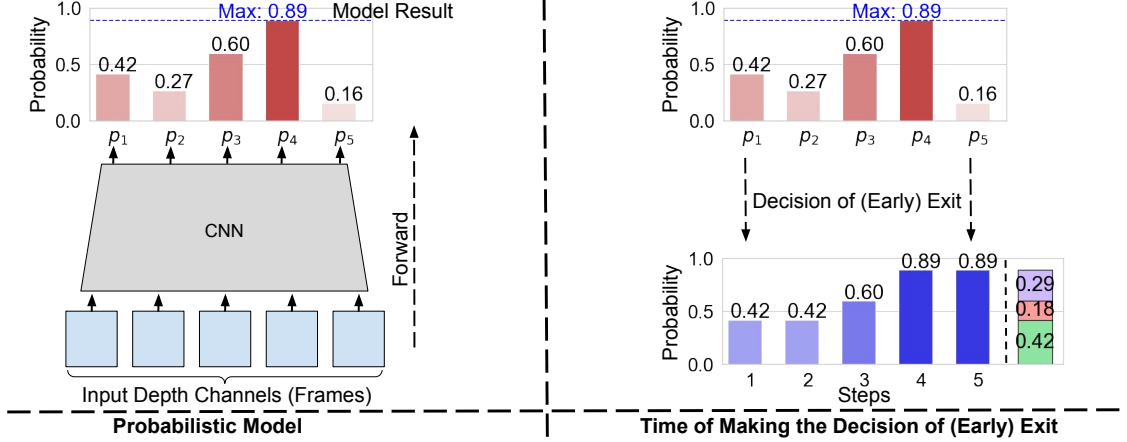


Figure 2: The left image illustrates a probabilistic model where the outcome is determined by selecting the maximum value of  $p_i$  (0.89 in this case). The right image shows an alternative approach where the model can terminate earlier based on available probabilities. For the example provided, the model exits with a probability of 0.42 at the 1st step, 0.18 at the 3rd step, and 0.29 at the 4th step.

exit and  $\infty$  when no early exit was made. We are interested in calculating the function  $\text{Exit}(V)$ , which represents the expected time of early exit (provided that it has been made). In order to achieve this, we define the random variable  $W = T_V | T_V < \infty$  with values from the set  $\{0, 1, \dots, n\}$  as follows: we draw a random variable  $\tau$  uniformly from the interval  $[0, \max_i p_i]$ , and for the given value of  $\tau$ , we return the first index  $k \in [0, n]$  for which  $p_k \geq \tau$ . Then we have

$$\mathbb{E}(W) = p(W \geq 1) + \dots + p(W \geq n) = n - P(V \leq 0) - \dots - P(V \leq n-1). \quad (3)$$

Finally, we get

$$\text{Exit}(V) = n - \frac{1}{\max p_i} \sum_{t=0}^{n-1} \max_{i=0..t} p_i \in [0, n] \quad \text{and} \quad \text{NE}(V) = \frac{1}{n} \text{Exit}(V) \in [0, 1]. \quad (4)$$

The function NE is defined as a normalization of  $\text{Exit}(V)$  with respect to the number of frames. It returns 0 if we have made the exit (with probability one) on the frame  $V_0$ , and 1 if we cannot exit before  $V_n$  and the probability of exit in  $V_n$  is positive.

**Loss function for PrAViC** Now we will describe how to incorporate the NE function into the loss function in a way that encourages the model to exit earlier. However, we do not want to stimulate the model too much so as not to provoke wrong decisions. To do this, we set a parameter  $\lambda \in [0, 1]$  that tells us how large a percentage of confidence we are willing to potentially sacrifice in order to make the decision early. Consider the videos  $\bar{V}, \tilde{V}$  from the positive class, where  $p(\bar{V}) = 1, \text{NE}(\bar{V}) = 1$  and  $p(\tilde{V}) = \tau, \text{NE}(\tilde{V}) = 0$ . Our goal is to add an additional part to the loss function in such a way that the loss of  $V$  and  $\tilde{V}$  is equal. Obviously  $\log(\lambda + (1 - \lambda)\text{NE}(\bar{V})) = \log(\lambda + (1 - \lambda)\text{NE}(\tilde{V}))$ .

Consequently, we define the objective for image  $V$  with class  $y \in \{0, 1\}$  as follows:

$$\text{loss}(V, y) = \text{BCE\_loss}(V, y) + y \log(\lambda + (1 - \lambda)\text{NE}(V)). \quad (5)$$

It is evident that for videos belonging to the negative class, the loss function remains the standard BCE loss. Conversely, for videos  $\bar{V}$  and  $\tilde{V}$  discussed above, we have  $\text{loss}(\bar{V}, 1) = \text{loss}(\tilde{V}, 1)$ . It is also noteworthy that for  $\lambda = 1$ , the additional part of the loss function is equal to 0, which discourages the model from making early decisions. As the value of  $\lambda$  approaches 0, the model is encouraged to make decisions as rapidly as possible, even if this results in a loss of accuracy.

## 4 Architecture of the model

In this section, we introduce the architecture of our proposed approach, detailing the modifications and enhancements made to the CNN-3D network. Our approach involves specific alterations to key layers, including the convolution layers and batch normalization, as well as a unique method for processing the network's head. Our architectural modifications aim to leverage the strengths of traditional CNN-3D networks while addressing specific challenges related to depth processing and feature extraction. The following sections provide a detailed breakdown of each component and its role within our approach.

**Architecture enabling fine-tuning** We outline the modifications made to the classic 3D CNN architecture to adapt it to our approach. While most components of a standard CNN architecture remain unchanged, we specifically alter the 3D convolution processing, batch normalization, and layer pooling. For 3D convolutions, we modify only those layers where the kernel size responsible for the depth (i.e., processing movie frames) is greater than 1. Our modification ensures that the kernels do not extend to the last deep channel. To achieve this, we replicate the input boundary on the front side before performing the multiplication operation, as illustrated in Fig. 3. For pooling layers, our modification involves replicating only the first depth channel.

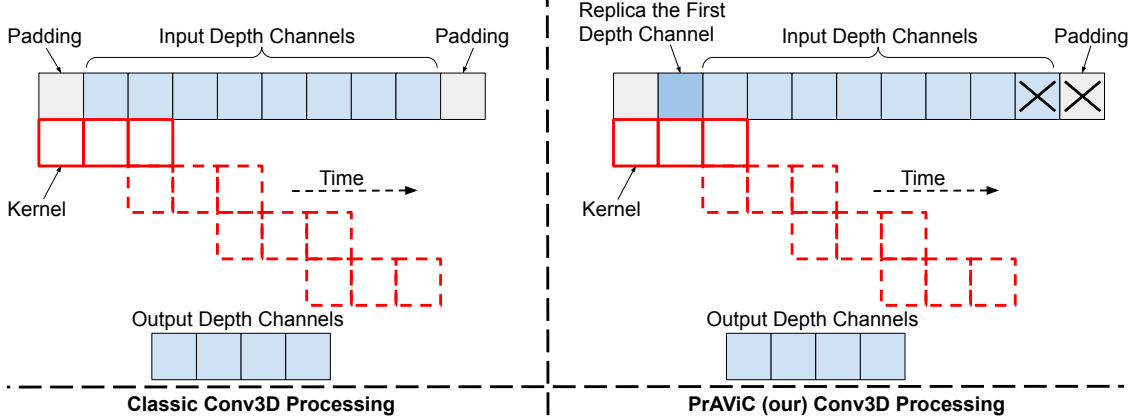


Figure 3: The picture illustrates the mechanism of the classic 3D convolution processing (left) with parameters: padding 1, stride 2, and kernel size 3, compared to our modified convolution processing (right). Note that the proposed change in input processing does not alter the kernel weights.

The next essential mechanism in CNN networks is batch normalization [6]. It involves calculating the mean and standard deviation for individual dimensions within mini-batches and training gamma and beta parameters during network training. This process ensures consistent and stable training across the network by maintaining the integrity of feature scaling and normalization, which is crucial for effective spatiotemporal pattern learning. In our approach, we modify this mechanism by statically determining the number of depth channels from which the statistics (mean and standard deviation) will be calculated. These statistics are then used to transform the remaining depth channels.

It’s important to note that through these operations, each layer of our model retains information from preceding depth channels only. Additionally, our approach possesses a unique property: when provided with inputs of the same movie, where one contains  $k$  frames and the other  $n$  frames ( $k < n$ , with the second input being an extension of the first by  $n - k$  frames), the network produces identical outputs, constricted to the dimensions of the output from the  $k$  first depth channels of inputs.

**Head design** Here, we describe the modifications to the head of the CNN network to enable online training and recursive evaluation as we show in Fig. 4. Typically, in the case of a CNN, the head consists of the final linear layer, so in our approach, we leave the head as a linear layer, but we will process the output from the last convolutional layer differently than it is done in a classic CNN network. We assume that  $v_0, \dots, v_n \in \mathbb{R}^D$  represent the outputs from the last convolutional and pooling layers, considering only the height and width dimensions while retaining the depth dimension as it is after the final convolutional layer. With this representation, following the standard offline approach, we perform one of the mean aggregation of representations relative to time  $t \in [0, \dots, n]$ :

$$w_t = \frac{1}{t+1} \sum_{i=0}^t v_i. \quad (6)$$

Using the above aggregations  $w_t$ , we process each separately through a linear layer  $h$  followed by the sigmoid  $\sigma$  function to obtain  $p_t = \sigma(h(w_t))$ . The final decision of the model is determined by the formula<sup>1</sup>  $p = \max_{t=0..n} p_t$ . The source code is available at <https://github.com/...>

<sup>1</sup>One can also use soft maximum given by  $p = (\frac{1}{n+1} \sum_{i=0}^n p_i^s)^{1/s}$  for parameter  $s \gg 1$ , which performs usually better in gradient optimization applications. Note that for the limiting  $s = \infty$ , we obtain a hard maximum.

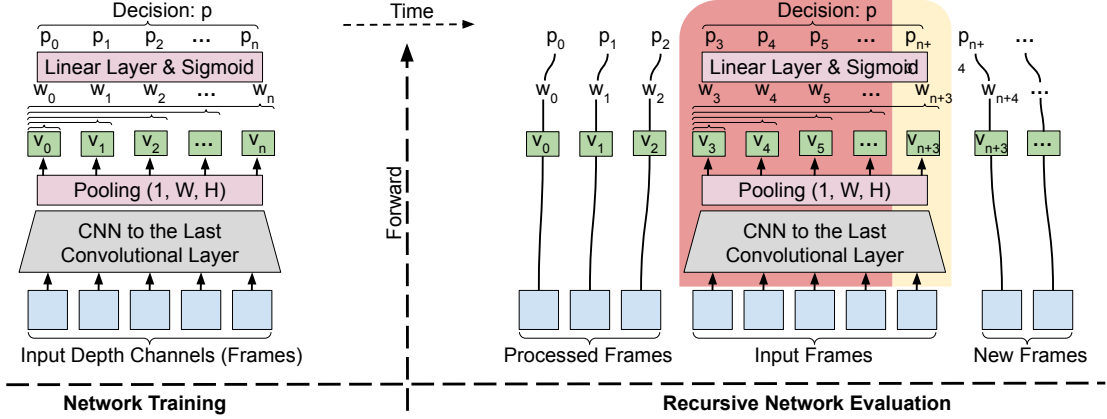


Figure 4: The picture depicts a diagram of the proposed approach during the training phase (left) and the recursive evaluation phase (right). In the model evaluation phase, the red area retains the computations from previous frames in individual network layers, while the yellow area represents the calculations for the newly added frame. Without retaining the computations in the red area, they would need to be recomputed, resulting in a longer evaluation process. This procedure allows for the rapid processing of new frames in an online manner.

## 5 Experiments

In this section, we detail the experimental setup and present the results that validate the effectiveness of our proposed approach. We utilized three datasets for testing: two publicly available (UCF101 [20] and EgoGesture [30]) and one closed-access (Ultrasound). Various architectures were employed in these experiments, each of which is described in the respective subsections. The numerical experiments were conducted using NVIDIA RTX 4090 and NVIDIA A100 40GB GPUs.

### 5.1 Comparison on UCF101 dataset

In this subsection we compare PrAViC with the baseline non-online approaches, ResNet-3D-18 (R3D-18) [21] and Separable-3D-CNN (S3D) [26]. We conduct experiments on widely used video benchmark, UCF101 [20]. This dataset

Table 1: Classification results on UCF101 dataset. R3D-18 and S3D are baseline non-online models. Our modifications applied to these models are indicated by PrAViC(name of the baseline model). PrAViC\*(name of the baseline model) indicates additional custom loss function (5). The third column presents the average decisive frame number i.e. number of the frame, on which the model made the classifying decision. The addition of a custom loss function forced both models to make decisions much earlier than models with categorical cross-entropy.

Model	offline		online			
	R3D-18	S3D	Best Accuracy		Best Time	
	R3D-18	S3D	PrAViC(R3D-18)	PrAViC(S3D)	PrAViC*(R3D-18)	PrAViC*(S3D)
<b>Accuracy(%)</b>	94.41	96.45	92.63	92.08	79.82	92.93
<b>Avg decisive frame</b>	16	16	11.71	9.71	7.06	6.03

is composed of 13320 videos from 101 action categories. These 101 categories fall into 5 subgroups: Body motion, Human-human interactions, Human-object interactions, Playing musical instruments, and Sports. Together, the video clips span over 27 hours. They are collected from YouTube, and uniformly recorded at 25 frames per second with a resolution of  $320 \times 240$ . Each video clip is labeled with a single action class. The dataset is partitioned into three sets: training, validation, and testing in a ratio of 6:1:1. From each video clip we extract 16 consecutive frames, starting with a random frame of a whole video clip, which enables such operation. For the R3D-18 model, we resize each frame to resolution  $128 \times 171$ , and randomly crop each frame to size  $112 \times 112$ . For the S3D model, we resize each frame to a resolution  $256 \times 256$  and randomly crop each frame to size  $224 \times 224$ .

First, we consider classic offline models for video classification: R3D-18 and S3D, which have been pre-trained on Kinetics-400 [9] dataset. We replaced number of outputs in the last layers to meet our classification problem with 101 distinct classes. Training took part in two stages. In the beginning, we trained just the last, classification layer for 5 epochs. After that, we fine-tune the entire network for 10 epochs. The batch size was set to 16 for both models. We use SGD optimizer. Learning rates for the first stage and second stage for R3D-18 were set to 0.01 and 0.0002, respectively. For S3D model: 0.01 and 0.0002, respectively. Cross entropy was the loss function.

Next, we modified R3D-18 and S3D networks as described in Sec. 4. Due to these changes, offline models became online. Same as previously, we replaced a number of outputs in the last layer of each model and training took part in two stages. In the first stage, we trained the last layer for 60 epochs. Fine-tuning was set up to 80 epochs. The batch size was set to 16 for both models. We use SGD optimizer. Learning rates for the first stage and second stage for modified R3D-18 were set to 0.002. For the S3D model: 0.015 and 0.0001, respectively. We report accuracy and number of decisive frames, i.e. number of frames, which on the first model was able to make a decision. Lastly, we applied a custom loss function as defined in (5). Our goal was to force the model to make an earlier decision. Various  $\lambda$  parameters were evaluated, starting with 0.1 up to 1.

In Tab. 1 we present classification results of baseline non-online models (R3D and S3D) and their online equivalents (PrAViC(R3D-18), PrAViC(S3D), PrAViC\*(R3D-18), PrAViC\*(S3D)) on UCF101 dataset. Our modified versions of baseline models are referred to as PrAViC(name of the baseline model), while PrAViC\*(name of the baseline model) denote additional custom loss function (5). Accuracies for PrAViC\*(name of the baseline model) models are chosen for the best  $\lambda$  parameter (for accuracies for different  $\lambda$  parameters see Fig. 5). Moreover, the best, across different  $\lambda$  parameters, the average decisive frame is listed for on-line models. By adding a custom loss function for PrAViC(name of the baseline model) networks, we achieved a decision speed approximately 1.5 times faster. For PrAViC\*(S3D)) model accuracy does not decrease significantly.

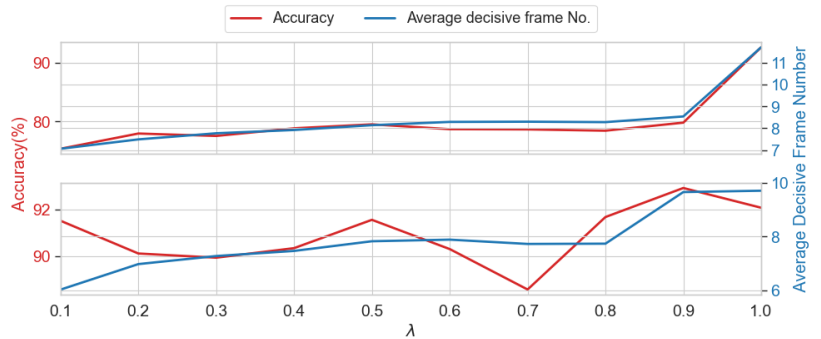


Figure 5: Comparison of accuracies and average decisive frame numbers depending on custom loss function parameter  $\lambda$ . First row presents results for PrAViC\*(R3D-18) and second row for PrAViC\*(S3D). The model has a tendency to delay decisions and have higher accuracy as the  $\lambda$  parameter values increase, contrasting with quicker decision-making and lower accuracy observed for lower parameter values. Observe that encouraging the model to make early decisions results in a small loss in accuracy.

Fig. 5 shows accuracies and averages decisive frame numbers for  $\lambda$  parameter varying from 0.1 up to 1. We observe increasing both accuracy and average decisive frame number, as the  $\lambda$  parameter rises.

## 5.2 Comparison on EgoGesture dataset

In this experiment, we harnessed a collection of trained models: 3D-SqueezeNet, 3D-ShuffleNetV1, 3D-ShuffleNetV2, and 3D-MobileNetV2, as outlined in [11]. These models were trained on the EgoGesture dataset [30], tailored for egocentric hand gesture recognition.

In setting up this experiment, we employ the learned model weights [11] on the data, initially training new model heads, followed by a light retraining of the entire model, with or without incorporating an additional cost function to promote earlier detection. The architectures used in our approach are the same as those of the base models, with modifications detailed in Sec. 4 of the paper. We utilize stochastic gradient descent (SGD) with standard categorical cross-entropy loss for training the architectures. The momentum, damping, and weight decay are configured as 0.9, 0.9, and 0.001, respectively. The network learning rate is initialized at 0.1, 0.05, and 0.01, then decreased by a factor of 3 with a factor of 0.1 when the validation loss reaches convergence.

During model training, input clips are selected from random time positions within the video clip. If the video comprises fewer frames than the input size, loop padding is implemented. For input into the network, we utilize clips with multiples of 16 frames. Specifically, for 3D-MobileNetV2, we use 128 frames, while for the remaining models, we utilize 192 frames. This approach is adopted to yield 8 probability values  $p_i$  at the network output for the MobileNet network and 12 for the other networks. A single input clip has dimensions of  $3 \times n \times 112 \times 112$ , where  $n$  represents the number of frames, varying based on the models used (as described above).

Table 2: The table presents the Top 1 (A@1) and Top 5 (A@5) accuracy results for both validation (val) and test sets of EgoGesture data. Base models are the best models trained on this dataset available at <https://github.com/ahmetgunduz/Real-time-GesRec>. The proposed PrAViC approaches are denoted as 'our' and 'our\*', where the star indicates the use of an additional cost function for earlier decision-making. Our approach, utilizing the same architectures with modifications described in Sec. 4, shows improved performance in most cases and supports online recursive usage (see Fig. 4).

Metric	Data Split	SqueezeNet			ShuffleNet			ShuffleNetV2			MobileNetV2		
		base	our	our*	base	our	our*	base	our	our*	base	our	our*
A@1	test	88.23	91.84	90.86	89.91	86.05	84.35	90.46	91.44	90.73	90.31	91.38	91.84
	val	84.25	87.14	86.16	85.77	82.12	80.01	85.83	86.60	85.17	86.28	86.56	87.50
A@5	test	97.63	99.20	99.16	98.28	99.10	99.18	98.36	99.29	99.20	98.22	99.20	99.33
	val	95.88	94.58	95.66	96.40	96.40	96.91	96.81	96.14	96.72	96.91	97.37	97.53

Tab. 2 provides a detailed performance comparison between the proposed PrAViC approach and the base models retrained on the EgoGesture dataset, highlighting Top 1 and Top 5 accuracy results for both validation and test sets. As observed from the table, the PrAViC approach generally outperforms the base models across most metrics. This improvement is evident in both Top 1 and Top 5 accuracy for both validation and test sets. Furthermore, our approach offers the added advantage of being applicable in an online, recursive manner, providing enhanced functionality and efficiency in practical applications (see Fig. 4 for a visual representation). These results underscore the effectiveness of the proposed modifications and highlight the potential of our approach to deliver superior performance in online gesture recognition tasks.

### 5.3 Comparison on Ultrasound dataset

In the subsequent experiment, the developed method was tested on a real dataset of Doppler ultrasound images representing short-axis and suprasternal views of newborns' hearts. These recordings were obtained as part of an ongoing scientific research project involving pediatric cardiologists, with the consent of the newborns' parents. During the acquisition process, a total of 18,365 ultrasound recordings were collected. The standard video analysis offline model trained on this dataset was modified by changing the classification layer (head) as well as the convolutional layers, in particular batch norm. These changes allowed for subsequent frames to be added sequentially while the model was running. These changes required fine-tuning of the model. Since the classification layer was completely new, fine-tuning started with 5 epochs of learning only this layer with a learning rate of  $10^{-5}$ . Subsequent training of this model for 10 epochs, with the same learning rate, but this time with training of all changed layers, allowed to achieve 94%. Standard Cross-entropy as a cost function was used in both stages.

Using our own cost function provided in Eq. (5), which prefers to classify as a class 1 element as quickly as possible, if it belongs to it, allowed us to achieve slightly lower accuracy as in the standard model, so approximately 90% regardless of the lambda parameter as in Tab. 3. Due to the model's use of remembered history, the model's accuracy was tested by introducing 16 frames into the model, i.e. the number needed for each convolutional layer inside the model to have at least one output representation other than padding. Only subsequent frames were added one at a time.

Table 3: Classification on Ultrasound Dataset with depending on custom loss function  $\lambda$  parameter. The model does not show much difference in accuracy depending on the  $\lambda$  parameter, because most decisions are made after processing the initial 16 frames anyway.

$\lambda$	0.1	0.2	0.3	0.4	0.5	0.6	0.7	0.8	0.9	1.0
<b>Accuracy(%)</b>	86.95	88.53	88.53	90.90	90.90	91.30	91.30	90.90	90.90	88.93

The model was then repeatedly evaluated on the selected video with different frame delivery parameters. The average time from 100 evaluations was taken as the result of the experiment for each set of parameters. The first parameter was the total number of frames delivered after all steps were completed. Due to the growing history in memory, it was expected that the increase in time would not be linear, i.e. 2 times as many frames should result in an evaluation more than 2 times longer. The experimental results confirmed this thesis. On the other hand, not single frames but entire batches can be loaded into the model. For this reason, in the second experiment, the first experiment was repeated, but instead of a single frame, 4 or 8 frames were fed to the model in each step. Thus, the history stored in the model worked



in the same way as before, but the number of reads and writes to it, was reduced. Due to the expected operation of the model on devices with lower performance, e.g. mobile devices, the first part of the tests were carried out on a CPU. The experiments were also repeated using the CUDA architecture. The results from both devices are presented in Fig. 6.

The conducted experiments have demonstrated the efficacy of the developed methodology in identifying congenital heart defects (CHDs) in neonates through ultrasound imaging. CHDs, encompassing conditions such as Tetralogy of Fallot, Hypoplastic Left Heart Syndrome, and Ventricular Septal Defect, pose formidable diagnostic hurdles owing to their intricate nature and the subtleties inherent in early cardiac anomalies. Regrettably, undetected instances of such defects represent a prominent contributor to neonatal mortality rates. The adapted video analysis model utilized in this investigation heralds a significant leap forward in the diagnostic realm pertaining to congenital heart defects.

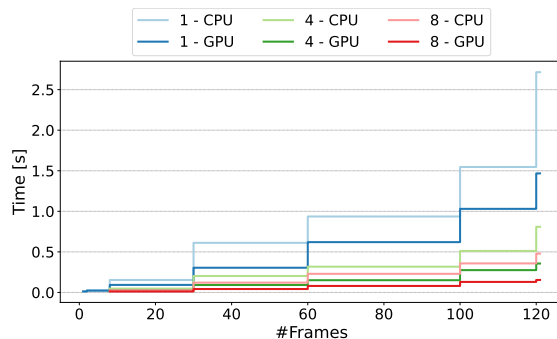


Figure 6: Model evaluation on time. Each line corresponds with the device used for evaluation and the number of frames inserted into the model in one step.

## 6 Conclusions

In this work, we propose PrAViC, a general framework to automatically modify networks adapted to the processing of the whole video, to their online counterpart. To do this we introduce the probabilistic theoretical model behind online data processing. This allows us to define the expected exit time and use it as a component of the loss function to encourage the model to make early decisions.

**Limitations** In PrAViC we use standard convolutions which have a time component. Although this allows the use of pre-trained networks, this does not allow the full use of the full frames of the video in the residual network, which can potentially lead to a small loss of accuracy.

**Broader impact** Since the use of online analysis of video is gaining importance in medical and social applications, our method can be applied as an easy-to-use tool for researchers working in applied video processing.

## References

- [1] Geetanjali Bhola and Dinesh Kumar Vishwakarma. A review of vision-based indoor har: state-of-the-art, challenges, and future prospects. *Multimedia Tools and Applications*, 83(1):1965–2005, 2024.
- [2] Joao Carreira and Andrew Zisserman. Quo vadis, action recognition? a new model and the kinetics dataset. In *proceedings of the IEEE Conference on Computer Vision and Pattern Recognition*, pages 6299–6308, 2017.
- [3] Shaopeng Chang and Xueyu Huang. Lm-net: a dynamic gesture recognition network with long-term aggregation and motion excitation. *International Journal of Machine Learning and Cybernetics*, 15(4):1633–1645, 2024.
- [4] Gongzheng Chen, Zhenghong Dong, Jue Wang, and Lurui Xia. Parallel temporal feature selection based on improved attention mechanism for dynamic gesture recognition. *Complex & Intelligent Systems*, 9(2):1377–1390, 2023.
- [5] Guan Huang, Son N Tran, Quan Bai, and Jane Alty. Real-time automated detection of older adults’ hand gestures in home and clinical settings. *Neural Computing and Applications*, 35(11):8143–8156, 2023.
- [6] Sergey Ioffe and Christian Szegedy. Batch normalization: Accelerating deep network training by reducing internal covariate shift. In *International conference on machine learning*, pages 448–456. pmlr, 2015.
- [7] Misha Karim, Shah Khalid, Aliya Aleryani, Jawad Khan, Irfan Ullah, and Zafar Ali. Human action recognition systems: A review of the trends and state-of-the-art. *IEEE Access*, 2024.
- [8] Michail Kaseris, Ioannis Kostavelis, and Sotiris Malassiotis. A comprehensive survey on deep learning methods in human activity recognition. *Machine Learning and Knowledge Extraction*, 6(2):842–876, 2024.
- [9] Will Kay, Joao Carreira, Karen Simonyan, Brian Zhang, Chloe Hillier, Sudheendra Vijayanarasimhan, Fabio Viola, Tim Green, Trevor Back, Paul Natsev, Mustafa Suleyman, and Andrew Zisserman. The kinetics human action video dataset, 2017.
- [10] Myeongjun Kim, Federica Spinola, Philipp Benz, and Tae-hoon Kim. A\*: Atrous spatial temporal action recognition for real time applications. In *Proceedings of the IEEE/CVF Winter Conference on Applications of Computer Vision*, pages 7014–7024, 2024.

- [11] Okan Köpüklü, Ahmet Gunduz, Neslihan Kose, and Gerhard Rigoll. Online dynamic hand gesture recognition including efficiency analysis. *IEEE Transactions on Biometrics, Behavior, and Identity Science*, 2(2):85–97, 2020.
- [12] Okan Köpüklü, Stefan Hörmann, Fabian Herzog, Hakan Cevikalp, and Gerhard Rigoll. Dissected 3d cnns: Temporal skip connections for efficient online video processing. *Computer Vision and Image Understanding*, 215:103318, 2022.
- [13] Adrian Krenzer, Michael Banck, Kevin Makowski, Amar Hekalo, Daniel Fitting, Joel Troya, Boban Sudarevic, Wolfgang G Zoller, Alexander Hann, and Frank Puppe. A real-time polyp-detection system with clinical application in colonoscopy using deep convolutional neural networks. *Journal of imaging*, 9(2):26, 2023.
- [14] Gautam Kumar. Average rolling based real-time calamity detection using deep learning, 2019. Accessed on May 20th, 2024.
- [15] Zhi Lu, Shiyin Qin, Pin Lv, Ligu Sun, and Bo Tang. Real-time continuous detection and recognition of dynamic hand gestures in untrimmed sequences based on end-to-end architecture with 3d densenet and lstm. *Multimedia Tools and Applications*, 83(6):16275–16312, 2024.
- [16] Yue Ming, Jiangwan Zhou, Nannan Hu, Fan Feng, Panzi Zhao, Boyang Lyu, and Hui Yu. Action recognition in compressed domains: A survey. *Neurocomputing*, page 127389, 2024.
- [17] Ali Mollahosseini, David Chan, and Mohammad H Mahoor. Going deeper in facial expression recognition using deep neural networks. In *2016 IEEE Winter conference on applications of computer vision (WACV)*, pages 1–10. IEEE, 2016.
- [18] Ade Iriani Sapitri, Siti Nurmaini, Muhammad Naufal Rachmatullah, Bambang Tutuko, Annisa Darmawahyuni, Firdaus Firdaus, Dian Palupi Rini, and Anggun Islami. Deep learning-based real time detection for cardiac objects with fetal ultrasound video. *Informatics in Medicine Unlocked*, 36:101150, 2023.
- [19] Yuqin Shen, Angli Chen, Xinsen Zhang, Xingwei Zhong, Ahuo Ma, Jianping Wang, Xinjie Wang, Wenfang Zheng, Yingchao Sun, Lei Yue, et al. Real-time evaluation of helicobacter pylori infection by convolution neural network during white-light endoscopy: a prospective, multicenter study (with video). *Clinical and Translational Gastroenterology*, 14(10):e00643, 2023.
- [20] Khurram Soomro, Amir Roshan Zamir, and Mubarak Shah. Ucf101: A dataset of 101 human actions classes from videos in the wild, 2012.
- [21] Du Tran, Heng Wang, Lorenzo Torresani, Jamie Ray, Yann LeCun, and Manohar Paluri. A closer look at spatiotemporal convolutions for action recognition, 2018.
- [22] İrem Üstek, Jay Desai, Iván López Torrecillas, Sofiane Abadou, Jinjie Wang, Quentin Fever, Sandhya Rani Kasthuri, Yang Xing, Weisi Guo, and Antonios Tsourdos. Two-stage violence detection using vitpose and classification models at smart airports. In *2023 IEEE Smart World Congress (SWC)*, pages 797–802. IEEE, 2023.
- [23] Zhengwei Wang, Qi She, and Aljosa Smolic. Action-net: Multipath excitation for action recognition. In *Proceedings of the IEEE/CVF conference on computer vision and pattern recognition*, pages 13214–13223, 2021.
- [24] Bichen Wu, Forrest Iandola, Peter H Jin, and Kurt Keutzer. Squeezedet: Unified, small, low power fully convolutional neural networks for real-time object detection for autonomous driving. In *Proceedings of the IEEE conference on computer vision and pattern recognition workshops*, pages 129–137, 2017.
- [25] Yi Xiao, Tong Liu, Yu Han, Yue Liu, and Yongtian Wang. Realtime recognition of dynamic hand gestures in practical applications. *ACM Transactions on Multimedia Computing, Communications and Applications*, 20(2):1–17, 2023.
- [26] Saining Xie, Chen Sun, Jonathan Huang, Zhuowen Tu, and Kevin Murphy. Rethinking spatiotemporal feature learning: Speed-accuracy trade-offs in video classification, 2018.
- [27] Chao Xu, Xia Wu, Mengmeng Wang, Feng Qiu, Yong Liu, and Jun Ren. Improving dynamic gesture recognition in untrimmed videos by an online lightweight framework and a new gesture dataset zjgesture. *Neurocomputing*, 523:58–68, 2023.
- [28] Jianhua Yang and Kun Dai. Yowov2: A stronger yet efficient multi-level detection framework for real-time spatio-temporal action detection. *arXiv preprint arXiv:2302.06848*, 2023.
- [29] Guangle Yao, Tao Lei, and Jiandan Zhong. A review of convolutional-neural-network-based action recognition. *Pattern Recognition Letters*, 118:14–22, 2019.
- [30] Yifan Zhang, Congqi Cao, Jian Cheng, and Hanqing Lu. Egogesture: a new dataset and benchmark for egocentric hand gesture recognition. *IEEE Transactions on Multimedia*, 20(5):1038–1050, 2018.

## APPENDIX / SUPPLEMENTAL MATERIAL

This section presents additional results that did not fit into the main part of the paper. These supplementary findings provide further insights and reinforce the conclusions drawn from our primary analyses. The results discussed here include analytical approaches and complementary experiments that offer a broader perspective on the research topic.

Based on the 3D-SqueezeNet model, we show the course of changes in the NE function while training this model. The image demonstrates these changes using the cost function (5) for  $\lambda = 1, 0.9, 0.5$ , respectively. As depicted in Fig. 7, with  $\lambda = 1$ , the NE value remains relatively stable, whereas a reduction in the  $\lambda$  parameter results in a more noticeable decline in the NE value, highlighting the effect of penalizing late detection on model performance.

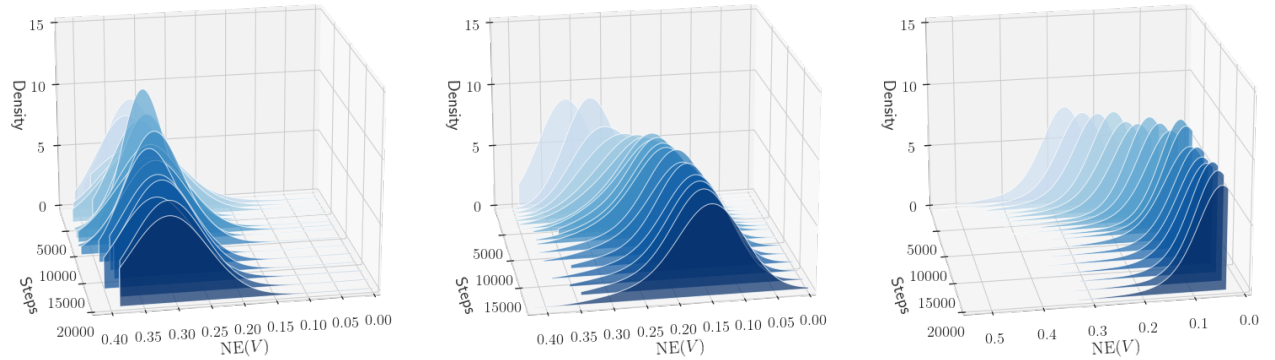


Figure 7: The image illustrates the progression of changes in the NE function (defined (4) in the main part of the paper) during the model 3D-SqueezeNet training process (from left to right) using the cost function (5) for  $\lambda = 1, 0.9$ , and  $0.5$ , respectively. For  $\lambda = 1$ , where late detection of classes is not penalized, the NE value remains relatively stable. However, as the  $\lambda$  parameter decreases, the NE value shows a more noticeable decline, indicating the increasing impact of penalizing late detection on the model’s performance.

Fig. 8 presents histograms of decisive frame numbers for PrAViC\*(R3D-18) and PrAViC\*(S3D) models (see Sec. 5.1 in main paper) with different  $\lambda$  parameters. The first row of the figure shows histograms for PrAViC\*(S3D), while the second row shows those for PrAViC\*(R3D-18). In both cases, we observe that larger  $\lambda$  values (depicted in deep blue shades) result in higher decisive frame numbers. Conversely, smaller  $\lambda$  values (depicted in white and light blue shades) lead the model to make decisions much earlier, as expected.

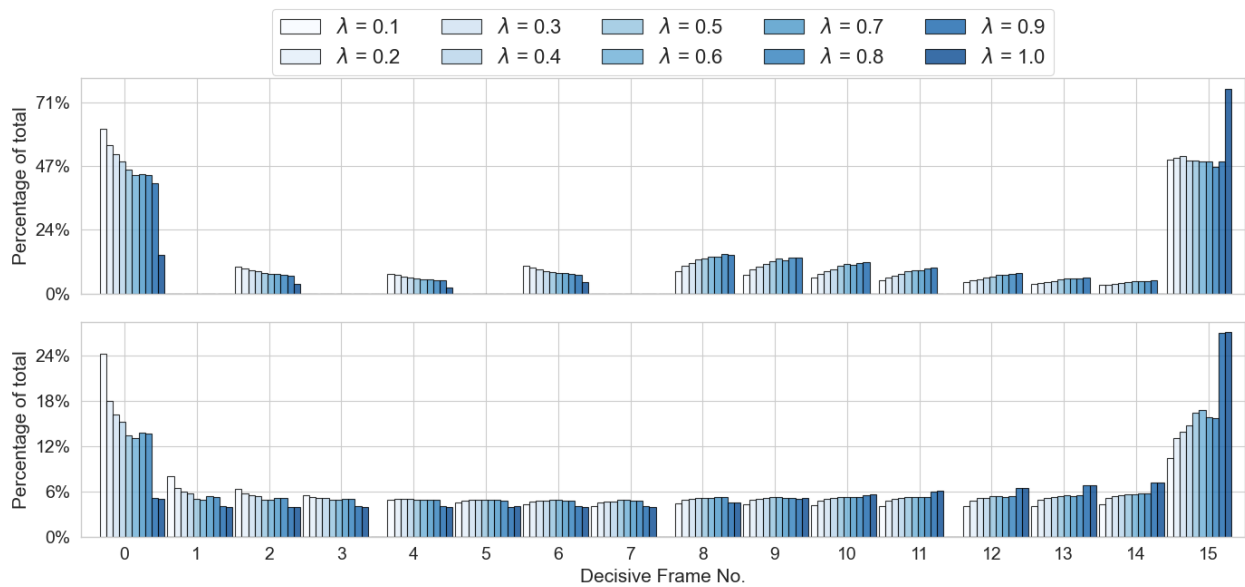


Figure 8: Comparison of histograms of decisive frame numbers for PrAViC\*(R3D-18)(first row) and PrAViC\*(S3D)(second row) models with different loss function  $\lambda$  parameters, varying from 0.1 to 0.9. The higher the  $\lambda$  value, the higher the percentage of higher numbers of decisive frames. Decreasing the  $\lambda$  parameter encourages the model to make decisions earlier.